JOURNAL OF Applied Polymer SCIENCE

Structure–property relationship of polyimide fibers containing ether groups

Jingjing Chang, Hongqing Niu, Min He, Meng Sun, Dezhen Wu
State Key Laboratory of Chemical Resource Engineering, College of Materials Science and Engineering, Beijing University of Chemical Technology, Beijing, China
Correspondence to: D. Wu (wdz@mail.buct.edu.cn)

ABSTRACT: The copolyimide (co-PI) fibers with outstanding mechanical properties were prepared by a two-step wet-spinning method, derived from the design of combining 4,4′-oxydianiline (ODA) with the rigid 3,3′,4,4′-biphenyltetracarboxylic dianhydride (BPDA)/*p*-phenylenediamine (*p*-PDA) backbone. The mechanical properties of PI fibers were drastically improved with the optimum tensile strength of 2.53 GPa at a *p*-PDA/ODA molar ratio of 5/5, which was approximately 3.7 times the tensile strength of BPDA/*p*-PDA PI fibers. Two-dimensional wide-angle X-ray diffraction indicated that the highly oriented structures were formed in the fibers. Two-dimensional small-angle X-ray scattering revealed the existence of the needle-shaped microvoids aligned parallel to the fiber axis, and the introduction of ODA led to the reduction in the size of the microvoids. As a result, the significantly improved mechanical properties of PI fibers were mainly attributed to the gradually formed homogeneous structures. The co-PI fibers also exhibited excellent thermal stabilities of up to 563°C in nitrogen and 536°C in air for a 5% weight loss and glass transition temperatures above 279°C.
 J. Appl. Polym. Sci. **2015**, *132*, 42474.

KEYWORDS: fibers; mechanical properties; morphology; polyimide; X-ray

Received 10 February 2015; accepted 6 May 2015
DOI: 10.1002/app.42474

INTRODUCTION

Owing to the outstanding mechanical properties, superior chemical and radiation resistance, excellent thermal stability, and good dielectric properties, aromatic polyimide (PI) fibers have been recognized as one of the most promising materials in the high-performance engineering materials.[1–4] Therefore, they are utilized in widespread fields such as electric, microelectronics, engineering, and aerospace applications.[5,6]

Among all the preparation systems, PI fibers derived from 3,3′,4,4′-biphenyltetracarboxylic dianhydride (BPDA) and *p*-phenylenediamine (*p*-PDA), known as Upilex-S type, are preferred due to the stiff and linear chain structure, strong intermolecular association, and high molecular orientation.[7–9] However, these features result in the poor processability of PI fibers simultaneously.[7,10] To overcome the drawback, the copolymerization with other flexible monomers has been found to be one of the most efficient approaches.[11–15] As reported by Huang *et al.*, a series of PI fibers containing 4,4′-oxydianiline (ODA) moieties were prepared via a dry-wet spinning method.[10] The processability and mechanical properties were improved significantly with the tensile strength and initial modulus up to 2.25 GPa and 96.5 GPa, respectively. Due to the low cost of ODA and the significantly improved mechanical properties of PI fibers, the monomer ODA was considered to be the ideal one to prepare high-performance PI fibers. Regrettably, the changes of aggregation state and morphology in the fibers after the introduction of ODA have not been systematically investigated, since the two factors generally exert considerable effects on the comprehensive performances of the resultant PI fibers.[16]

Inspired by the known success, with the purpose of obtaining high-performance PI fibers, in the present work, a series of copolyimide (co-PI) fibers derived from BPDA, *p*-PDA, and ODA were prepared via a two-step wet-spinning method. Herein, two-dimensional wide-angle X-ray diffraction (2D WAXD) and two-dimensional small-angle X-ray scattering (2D SAXS) were carried out to explore the variation of aggregation state and morphology with the increased ODA contents in the fibers. In addition, the effects of the incorporated ODA moieties on the thermal properties of the co-PI fibers were also discussed.

EXPERIMENTAL

Materials

The monomer BPDA was purchased from Shi Jiazhuang Hai Li Chemical Company and purified by sublimation. The monomers *p*-PDA and ODA were obtained from Shangyu Li Xing Chemical Company and purified by recrystallization. The

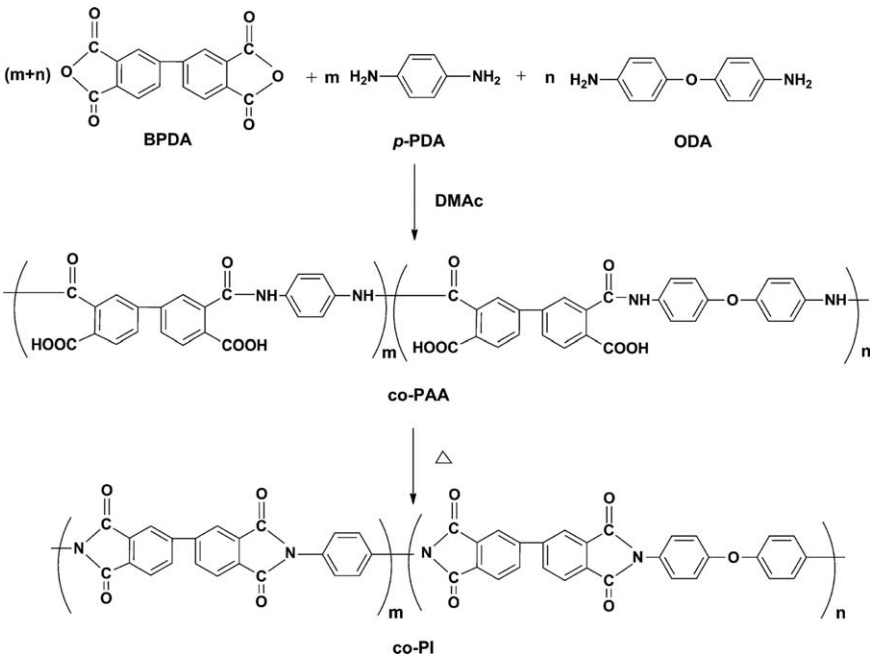

Scheme 1. The reaction of the preparation of the co-PAA and co-PI fibers. $m/n = 10/0$, 9/1, 8/2, 7/3, 6/4, 5/5.

solvent dimethylacetamide (DMAc) (analytical pure) was purchased from Tianjin Fu Chen Chemicals Reagent Factory and utilized after distillation. The deionized water used in the experiment was prepared by the Laboratory Water Purification System.

Preparation of the BPDA/p-PDA/ODA (BPO) co-PI Fibers

The co-PI fibers were prepared by the two-step wet-spinning method in the following procedures. Take the polycondensation of BPO-2 copoly(amic acid) (co-PAA) solution (the molar ratio of *p*-PDA/ODA is 8/2) for example, *p*-PDA (34.18 g) and ODA (15.82 g) were firstly dissolved in 1000 mL DMAc solvent by stirring under a dried atmosphere, and equimolar dianhydride BPDA (116.23 g) was added subsequently. The solution was stirred at a low temperature to obtain a spinning solution containing 15 wt % solid content. The viscous solution, filtrated and degassed prior to use, was extruded into the coagulation bath through a spinneret (100 holes, 70 μm in diameter) to get as-spun PAA fibers under the pressure of nitrogen. After washed by deionized water to remove the residual solvent DMAc, the PAA fibers were dried with the oven at the temperature of 80°C, and then were delivered into ovens with the temperatures ranging from 280°C to 500°C with concomitant drawing on the spinning rollers. The mechanical properties of PI fibers were improved extensively through the thermal imidization process. All the co-PI fibers with the molar ratios of *p*-PDA/ODA ranging from 10/0 to 5/5 were prepared under the same conditions. The reaction of the preparation of BPDA/*p*-PDA/ODA co-PAA and co-PI fibers is illustrated in Scheme 1.

Characterization

The Fourier transform infrared (FT-IR) measurements were carried out on Nexus 670 made by Nicolet Company with the scanning wavenumber ranging from 4000 to 400 cm^{-1} and average 32 scans. The samples were prepared by grinding the fibers with KBr in the mortar, and the measurements were conducted in the ambient atmosphere.

The intrinsic viscosities of the co-PAA solutions were measured using a Germany SCHOTT 52510 Ubbelohde viscometer at 35°C. For convenience, the intrinsic viscosities of the co-PAA solutions were acquired by a typical "one-point method".[17]

The mechanical properties of PI fibers were conducted on an Instron 3344 instrument with a gauge length and extension speed of 250 mm and 125 mm/min, respectively. For each group of fibers, at least 15 filaments were tested and the average value was used as the representative.

2D WAXD was performed on a Bruker D8 Discover diffractometer equipped with GADDS as a 2D detector. X-ray diffraction measurements were taken from reflection mode at room temperature using Ni-filtered Cu Kα ($\lambda = 0.154$ nm) radiation operated at 40 kV and 40 mA. According to the WAXD patterns, the degree of molecular orientation can be calculated by integrating the corresponding intensity of azimuthal scans along the isolated and preferred crystalline plane.[18] The degree of molecular orientation of the fibers is calculated based on the Hermans equation:

$$f = (3 < \cos^2\phi > -1)/2 \quad (1)$$

where f is the degree of molecular orientation along the fiber axis direction and ϕ represents the angle between the fiber axis and *c*-axis crystal unit cell. The numerical values of the mean-square cosines in the equation above are determined by corrected intensity distribution $I(\phi)$ diffracted from the crystalline plane by Gaussian fitting following the equation:

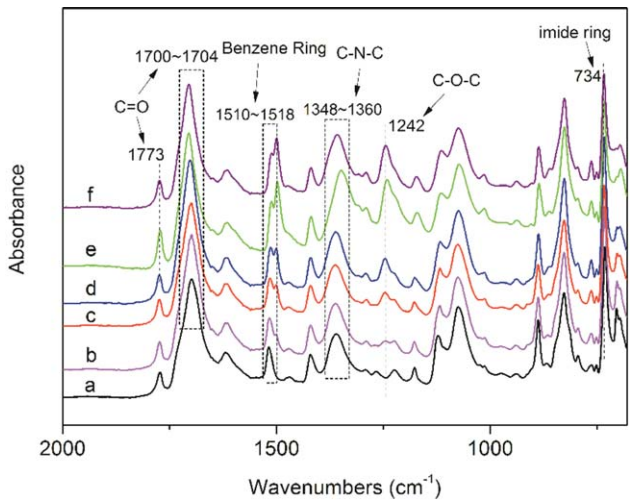

Figure 1. FT-IR curves of the co-PI fibers with different molar ratios of *p*-PDA/ODA. (a) BP-0; (b) BPO-1; (c) BPO-2; (d) BPO-3; (e) BPO-4; and (f) BPO-5. [Color figure can be viewed in the online issue, which is available at wileyonlinelibrary.com.]

$$<\cos^2\phi> = \frac{\int_0^{\pi/2} I(\phi)\sin\phi\cos^2\phi\, d\phi}{\int_0^{\pi/2} I(\phi)\sin\phi\, d\phi} \quad (2)$$

2D SAXS was performed on NanoSTAR-U (BRUKER AXS INC) using an HI-STAR detector. The generator was operated at 40 kV and 650 μA with Cu Kα radiation. The distance between the sample and the detector was $L_{SD} = 1074$ mm. The effective scattering vector q ($q = 4\pi\sin\theta/\lambda$, where 2θ is the scattering angle) at this distance ranging from 0.044 to 2.0 nm^{-1}. As for wet-spinning process, the needle-shaped microvoids along the fiber axial direction were characterized by SAXS. The radius of the microvoids can be described by Guinier functions as follows:

$$I(q) = I_0 \exp\left(\frac{-q^2R^2}{5}\right) \quad (3)$$

where R is the radius of the microvoids with circle cross-section and $I(q)$ is the scattering intensity in reciprocal. Through the Fankuchen successive tangent method, the average radius of the microvoids can be calculated according to the equation:

$$R = \sum R_i W_i (i = 1, 2, 3 \ldots) \quad (4)$$

where R_i is the radius of different size of the microvoids and W_i is the corresponding volume percentage of the microvoids.

Then, the average fibril length L and misorientation width B_Φ are determined by the following equation proposed by Ruland:

$$s^2 {B_{obs}}^2 = \frac{1}{L^2} + s^2 {B_\phi}^2 \quad (5)$$

where B_{obs} is the angular spread of the data fitting by Gaussian–Gaussian function and s is the scattering vector ($s = 2\sin\theta/\lambda$).

Thermogravimetric analyses (TGA) were performed with a TGA Q50 instrument at a heating rate of 10°C/min from 50 to 900°C. The samples weighing about 5.0 mg were tested in nitrogen and air.

Dynamic mechanical analyses (DMA) were employed on a DMA Q800 system with a load frequency of 1 Hz and heating rate of 5°C/min at the temperature from 50 to 450°C.

RESULTS AND DISCUSSION

FT-IR Spectra of the co-PI Fibers

The chemical structures of the co-PI fibers with different molar ratios of *p*-PDA/ODA were confirmed by FT-IR as shown in Figure 1. Four characteristic absorption bands of the co-PI fibers are observed at 1773, 1700–1704, 1348–1360, and 734 cm^{-1}, which are attributed to the C═O asymmetrical stretching of imide groups, C═O symmetrical stretching of imide groups, C—N stretching and C═O bending of imide ring, respectively.[19] In the region of 2000–600 cm^{-1}, the absorption bands of PAA fibers at 1660 cm^{-1} (amide-I band) and 1550 cm^{-1} (amide-II band) are not identified for all the fibers, suggesting the complete imidization of PI fibers in the two-step wet spinning method. In addition, the absorption bands at 1242 cm^{-1} are accounted for C—O—C stretching. The intensities of C—O—C absorption bands increase simultaneously with the increased ODA contents, indicating that the ether groups have been combined into the polymer backbone.

Mechanical Properties of the co-PI Fibers

The intrinsic viscosities of the co-PAA solutions and mechanical properties of corresponding co-PI fibers with different molar ratios of *p*-PDA/ODA are presented in Table I, while the stress-strain curves of the co-PI fibers are plotted in Figure 2. For homo-PI (BP-0) fibers, the fibers exhibit the tensile strength of 0.69 GPa, initial modulus of 62.1 GPa with elongation of 1.21%. With the introduction of ODA, the mechanical properties of the co-PI fibers improve drastically. The optimum mechanical properties are obtained for the BPO-5 fibers, which exhibit the tensile

Table I. The Intrinsic Viscosities of the co-PAA Solutions and Mechanical Properties of the Corresponding co-PI Fibers with Different Molar Ratios of *p*-PDA/ODA

PI fibers	Molar ratio of *p*-PDA/ODA	[η] (dL/g)	Tensile strength (GPa)	Initial modulus (GPa)	Elongation (%)
BP-0	10/0	2.32	0.69 ± 0.07	62.10 ± 1.90	1.21 ± 0.11
BPO-1	9/1	2.81	1.34 ± 0.13	89.76 ± 5.02	1.65 ± 0.13
BPO-2	8/2	2.69	1.77 ± 0.08	67.54 ± 2.61	3.25 ± 0.09
BPO-3	7/3	2.53	1.84 ± 0.07	60.42 ± 1.47	3.93 ± 0.18
BPO-4	6/4	2.49	2.30 ± 0.11	56.40 ± 1.94	5.80± 0.20
BPO-5	5/5	2.71	2.53 ± 0.14	53.10 ± 2.90	7.76 ± 0.27

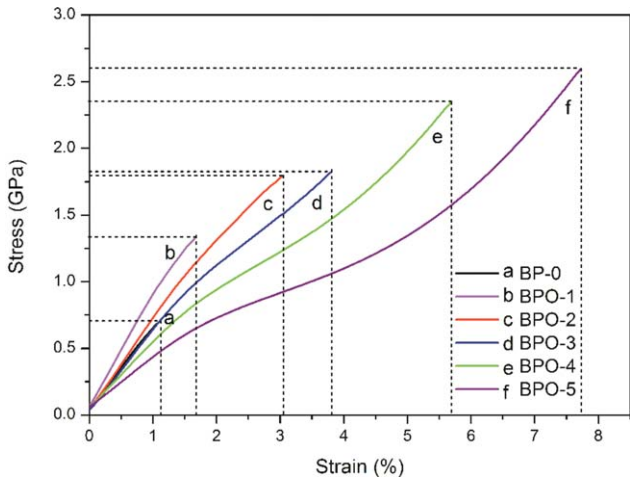

Figure 2. The stress–strain curves of the co-PI fibers. [Color figure can be viewed in the online issue, which is available at wileyonlinelibrary.com.]

strength of 2.53 GPa, initial modulus of 53.10 GPa, and elongation of 7.76%. Herein, the initial modulus of BPO-1 fibers shows a drastic increase as compared with that of homo-PI fibers, while further introducing the ODA contents leads to the decrease in the modulus oppositely. The variation in initial modulus of the PI fibers is mainly attributed to the improved flexibility of polymer chains. Due to the high rigidity of BPDA/*p*-PDA chains, the brittle homo-PI fibers are easily broken before showing the real capability of resisting external forces. However, the addition of ODA provides opportunities for PI fibers to obtain large deformation to arrange the polymer chains, giving evidence of the enhancement in the modulus of the fibers as compared with the modulus of BP-0 fibers. Meanwhile, further introduction of the ODA contents will inevitably result in the decreased rigidity of polymer chains. As a result, the modulus increases initially and then decreases along with the incorporation of the ODA contents. Moreover, the tensile strength and elongation of the co-PI fibers improve remarkably with the increased ODA contents, and the possible reasons for the improvement are inferred as follows. Generally, the mechanical properties of PI fibers depend on the intrinsic viscosity, rigidity of polymer backbone, intermolecular association, molecular orientation and structural defects.[13,15,20] As shown in Table I, the intrinsic viscosities of the co-PAA solutions vary in disorder with the incorporated ODA contents, which implies that the improved mechanical properties are not affected by intrinsic viscosities. Besides, the incorporation of the ODA contents has not introduced any intermolecular associations in the formation of chemical structures of PI fibers. Therefore, it is speculated that the enhancement in mechanical properties of PI fibers is attributed to the molecular orientation and structural evolution. In addition, the incorporation of ODA could possibly increase the chain entanglement and toughness of the resulting PI fibers owing to the improved flexibility of the polymer chains, which may also be responsible for the improvement in mechanical properties of the co-PI fibers.[21–23]

Molecular Packing of the co-PI Fibers

To evaluate the effect of crystallinity and molecular orientation on the final performance of PI fibers, the 2D WAXD patterns of the co-PI fibers with different molar ratios of *p*-PDA/ODA are obtained in Figure 3. The fibers exhibit clear diffraction streaks on the meridian direction, revealing the regular arrangement along the fiber axis. On the equator, the diffractions become much more diffuse with the incorporation of the ODA contents, indicating the poor lateral packing order along the transverse

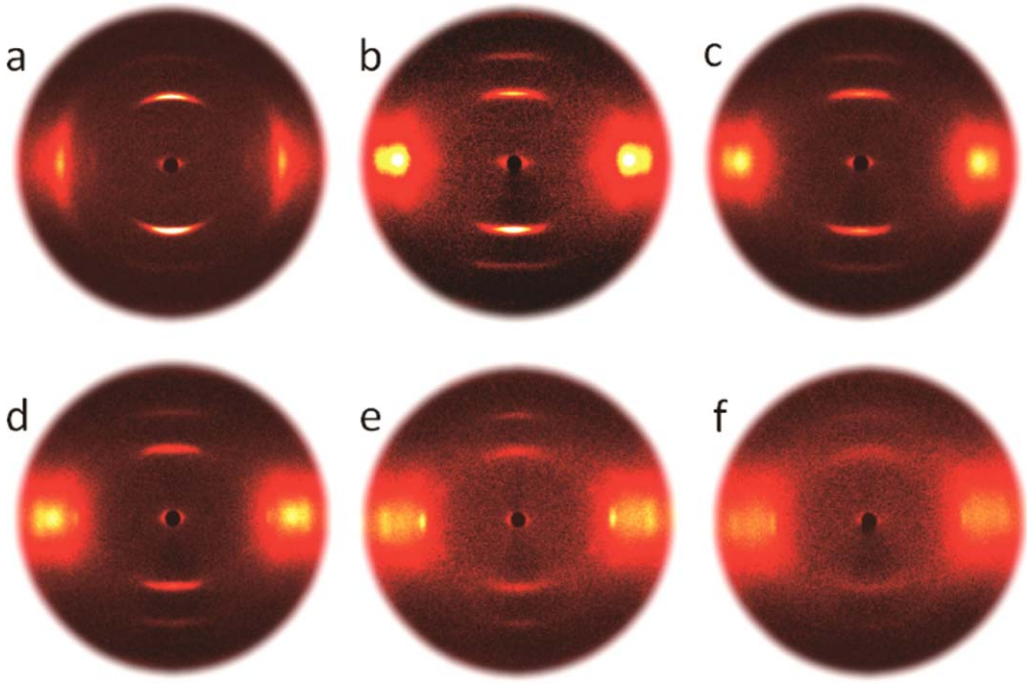

Figure 3. 2D WAXD patterns of the co-PI fibers with different molar ratios of *p*-PDA/ODA. (a) BP-0; (b) BPO-1; (c) BPO-2; (d) BPO-3; (e) BPO-4; and (f) BPO-5. [Color figure can be viewed in the online issue, which is available at wileyonlinelibrary.com.]

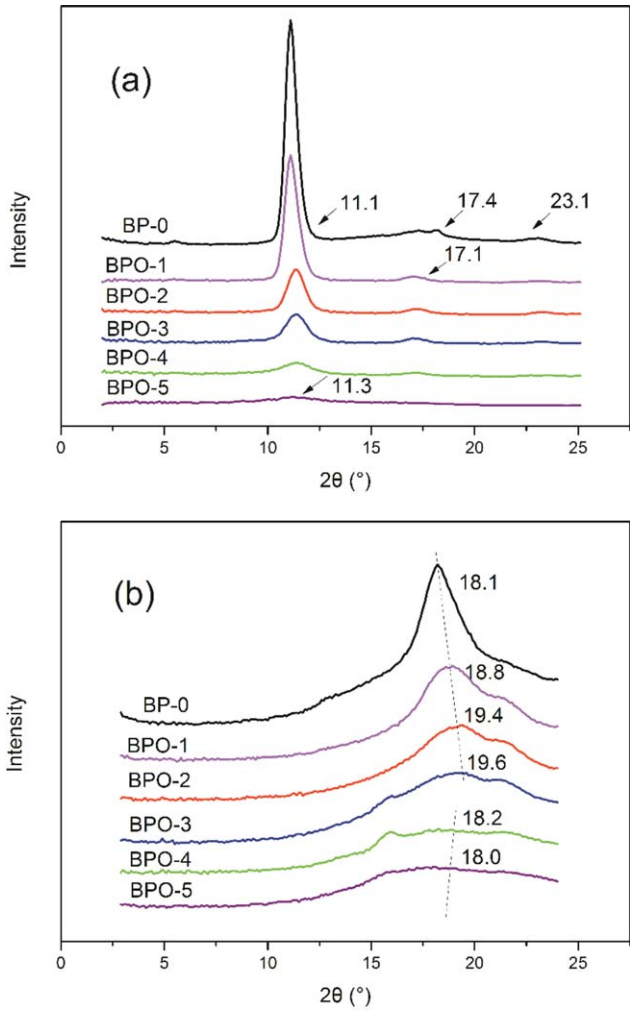

Figure 4. WAXD profiles of the co-PI fibers with different molar ratios of *p*-PDA/ODA. (a) Meridian direction and (b) equator direction. [Color figure can be viewed in the online issue, which is available at wileyonlinelibrary.com.]

direction of the fibers. Furthermore, the co-PI fibers do not exhibit well-defined 3D crystalline structures, since there is no evidence of diffractions in the quadrants.

Dramatic changes occur in the 2D WAXD patterns after the incorporation of the ODA contents. Figure 4(a) displays the WAXD profiles of the co-PI fibers along the meridian direction. For homo-PI fibers, three diffraction peaks at 11.1° ($d = 0.796$ nm), 17.4° ($d = 0.509$ nm) and 23.1° ($d = 0.385$ nm) are observed. In the previous work, the lowest energy conformation for BPDA/*p*-PDA units was obtained as a repeat length of 1.587 nm.[11] The value is close to the twice of the observed data at $2\theta = 11.1°$ ($0.796 \times 2 = 1.592$ nm) and the diffraction peak is set to be the (002) plane. Therefore, the peak at $2\theta = 17.4$ and 23.1° can be assigned to be (003) and (004) plane, respectively. After the introduction of ODA, the streak at 11.1° gradually shifts to high angle, and it reaches 11.3° for the fibers with molar ratio of *p*-PDA/ODA = 5/5. The slightly increased angles indicate that the incorporation of ODA results in the decrease of the ordered chain repeat length, since the flexibility of polymer chains has been increased after replacing some BPDA/*p*-PDA units with BPDA/ODA units. Compared with those of homo-PI fibers, the peaks at $2\theta = 17.4°$ and 23.1° gradually disappear with the increased ODA contents, revealing the gradually loss of ordered structures along the fiber axis.

In the equator regions as depicted in Figure 4(b), a series of broad diffraction peaks are observed at 18.1°, 18.8°, 19.4°, 19.6°, 18.2°, and 18.0°, corresponding to BP-0, BPO-1, BPO-2, BPO-3, BPO-4, and BPO-5 fibers, respectively. In contrast with that of homo-PI fibers, the peak becomes much more broad and diffuse with the increased ODA contents, especially for BPO-4 and BPO-5 fibers, showing the gradually loss of ordered and compact lateral packing structures.

In addition, the degree of molecular orientation has also been studied through WAXD, and the degree of molecular orientation of the (002) plane was calculated using eqs. (1) and (2). According to the results in Table II, the degree of molecular orientation increases to 0.91 at a *p*-PDA/ODA molar ratio of 9/1, while the further introduction of ODA leads to the drastically decrease in the degree of molecular orientation. The reduced degree of molecular orientation can be ascribed to the improved flexibility of polymer chains, which destroys the arrangement of molecular chains along the fiber axis. In conclusion, it can be implied that the enhancement in mechanical properties is not mainly affected by molecular orientation.

Morphologies of the co-PI Fibers

In the two-step wet-spinning method, due to the removal of micromolecules, some defects such as microvoids could generate during the dual diffusion and thermal imidization process, which has greatly affected the mechanical properties of PI fibers. In order to explore the parameters of microvoids, for instance, the average radius *R*, length *L*, and misorientation B_Φ, SAXS has become an ideal tool to investigate the structural change in the fibers. Generally, the scattering in SAXS contains several contributions including the microfibrillar structures and microvoids of the fibers.[24] From the 2D SAXS patterns of the co-PI fibers with different molar ratios of *p*-PDA/ODA as shown Figure 5, the microfibrillar scattering shows very weak intensity, and thus it can be concluded that the scattering is mainly due to the existence of microvoids in the fibers. The elongated shape of the streaks indicates that the microvoids are needle shaped and aligned parallel to the fiber direction.[25] Moreover, in the meridian direction of SAXS patterns, there are detectable scatterings for BPO-2 and BPO-3 fibers, suggesting the presence of periodic lamellar structures between crystalline and amorphous regions. However, with the increased ODA contents, the scattering streaks become much weaker and gradually disappear at a

Table II. The Calculated Degree of Molecular Orientation of the co-PI Fibers

PI fibers	BP-0	BPO-1	BPO-2	BPO-3	BPO-4	BPO-5
Degree of orientation	0.87	0.91	0.85	0.82	0.81	0.72

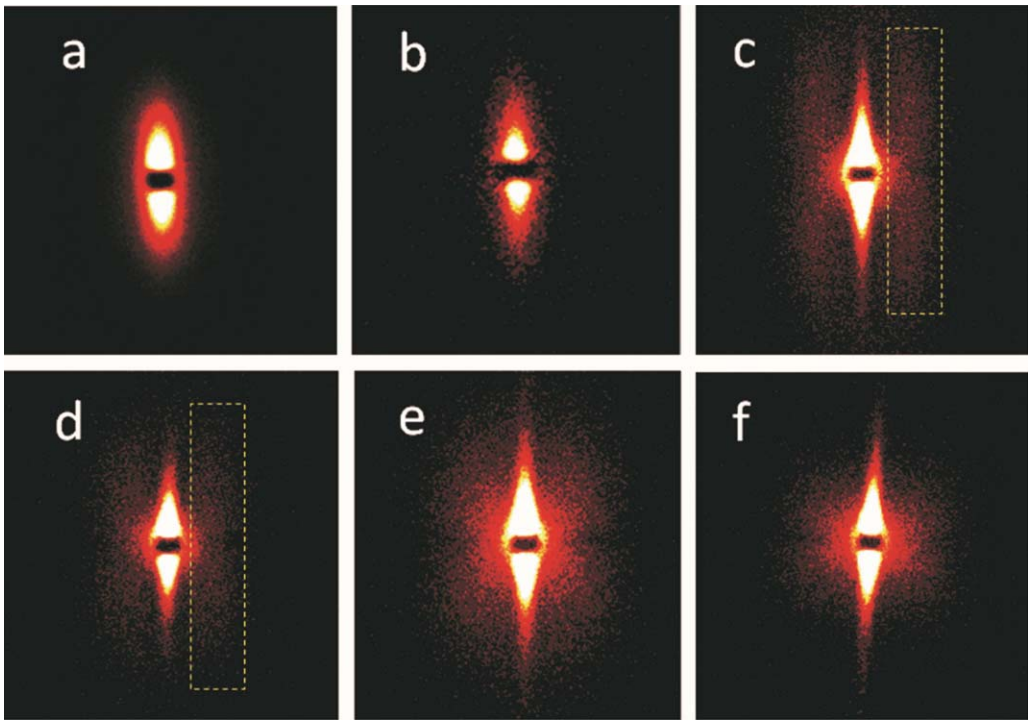

Figure 5. 2D SAXS patterns of the co-PI fibers with different molar ratios of *p*-PDA/ODA. (a) BP-0; (b) BPO-1; (c) BPO-2; (d) BPO-3; (e) BPO-4; and (f) BPO-5. [Color figure can be viewed in the online issue, which is available at wileyonlinelibrary.com.]

p-PDA/ODA molar ratio of 6/4, revealing the gradually loss of ordered packing structures in the polymer chains.

Figure 6 illustrates the SAXS profiles of the co-PI fibers along the meridian direction, and the strong scattering intensity near the beamstop indicates the existence of the microvoids. According to the study by Jiang *et al.*, the radius of microvoids correlates with the Guinier functions as displayed in eq. (3).[26,27] The radius R_i ($i = 1, 2, 3$) and corresponding volume percentage W_i ($i = 1, 2, 3$) to different size of microvoids can be confirmed by Fankuchen successive tangent method.[16] Thus, the average radius R of microvoids can be calculated according to eq. (4),

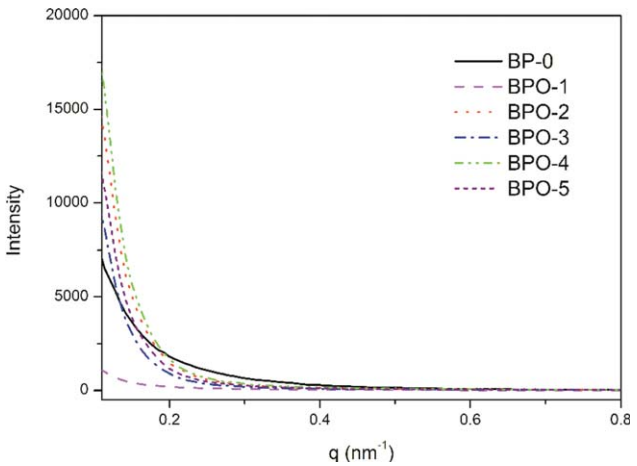

Figure 6. SAXS profiles of the co-PI fibers along the meridian direction. [Color figure can be viewed in the online issue, which is available at wileyonlinelibrary.com.]

and the results are listed in Table III. The introduction of ODA leads to the significant decrease in the radius of microvoids, and among all the fibers, the BPO-5 fibers have the smallest value of the average radius, implying that the gradually formed homogeneous structures could provide excellent performance for PI fibers. Moreover, both the size distribution and misorientation of microvoids have contributed to the streak profile as reported by Ran *et al.*[24] The average fibril length L and misorientation B_Φ could be calculated by eq. (5) proposed by Ruland.[28] The length L is obtained from the intercept of the $s^2B_{obs}{}^2$ vs. s^2 plot and misorientation B_Φ from the slope of the plot, while the Ruland plot of the BP-0 fibers is given in Figure 7. From the data in Table III, the fibril length and misorientation have also decreased dramatically upon the introduction of ODA. In all the fibers, the volume of microvoids for BPO-5 fibers is the lowest, and thus the fibers exhibit most homogeneous structures to resist external forces, showing the best mechanical properties in the series of co-PI fibers. Above all, due to the improved flexibility of polymer chains by incorporating ODA into the polymer backbone, the size of microvoids decreases drastically to form homogeneous structures in the fibers, resulting in outstanding mechanical properties of PI fibers.

Thermogravimetric Properties of the co-PI Fibers

Figure 8 illustrates the TGA curves of the co-PI fibers with the temperature ranging from 50 to 900°C at a heating rate of 10°C/min in nitrogen and air. The fibers exhibit similar behaviors in both nitrogen and air atmospheres, however, the fibers are much easier oxidized in air, demonstrating the sensitivity of thermal-oxidative stability of PI fibers to the atmosphere.

Table III. The Parameters of Microvoids of the co-PI Fibers Prepared with Different Molar Ratios of *p*-PDA/ODA

	R_i								
PI fibers	R_1 (nm)	W_1	R_2 (nm)	W_2	R_3 (nm)	W_3	*R* (nm)	*L* (nm)	B_Φ (°)
BP-0	3.10	1.00	0.36	0.17	0.16	0.33	3.62	113.19	28.17
BPO-1	2.55	1.00	0.30	0.11	0.20	0.06	3.05	110.42	25.09
BPO-2	2.56	1.00	0.27	0.09	0.17	0.05	3.00	109.50	22.81
BPO-3	2.24	1.00	0.27	0.09	0.13	0.04	2.64	103.18	21.14
BPO-4	2.09	1.00	0.16	0.05	0.10	0.03	2.35	100.86	19.31
BPO-5	1.73	1.00	0.17	0.07	0.11	0.05	2.01	93.46	13.31

Apparently, the homo-PI fibers exhibit the 5% weight loss temperature of 612°C and 606°C in nitrogen and air, respectively. After the introduction of ODA, the temperatures are in the region of 563–596°C in nitrogen and 536–586°C in air, resulting in the reduction of the thermal-oxidative stability of PI fibers. It is attributed to the increased C—O bonds in the polymer chains because the C—O bonds are much easier broken as compared with that of C—C bonds. Therefore, the fibers are much easier oxidized with the incorporation of ODA moieties. Nevertheless, the 5% weight loss temperatures increase to 596°C in nitrogen and 586°C in air for BPO-4 fibers, which are much higher than those of the other co-PI fibers. It can be attributed to the gradually formed homogeneous structures in the fibers at a *p*-PDA/ODA molar ratio of 6/4. In conclusion, the fibers exhibit excellent thermal-oxidative stabilities with the 5% weight loss temperatures above 563°C and 536°C in nitrogen and air, respectively.

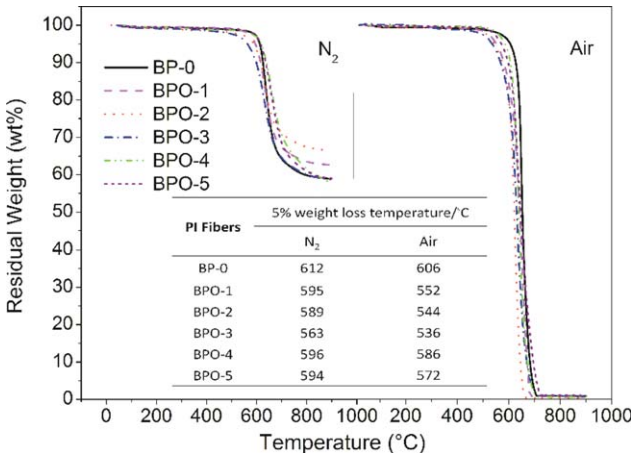

Figure 8. TGA curves of the co-PI fibers with different molar ratios of *p*-PDA/ODA in nitrogen and air. [Color figure can be viewed in the online issue, which is available at wileyonlinelibrary.com.]

Dynamic Mechanical Properties of the co-PI Fibers

Figure 9 shows the DMA curves of the co-PI fibers with the temperature ranging from 50 to 450°C at a heating rate of 5°C/min in nitrogen. Among all the curves, two series of peaks are observed. The higher ones are α relaxations, and the peaks of α relaxations correspond to the glass transition temperatures (T_g) of the polymer chains. The other ones are β relaxations corresponding to subglass transition of the PI fibers. For homo-PI fibers, the fibers exhibit the T_g value of 339°C, whereas the value decreases to 322, 305, 297, 286, and 279°C for BPO-1, BPO-2, BPO-3, BPO-4, and BPO-5 fibers, respectively. Meanwhile, the intensities of α relaxations increase drastically upon the introduction of ODA. It is known that α relaxations peaks refer to the energy consumption of the segmental motion in the amorphous regions in the materials. The decreased T_g values

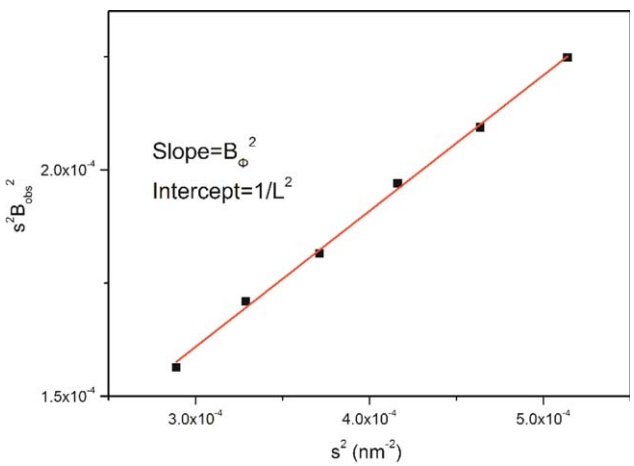

Figure 7. Ruland plot of the BP-0 fibers. [Color figure can be viewed in the online issue, which is available at wileyonlinelibrary.com.]

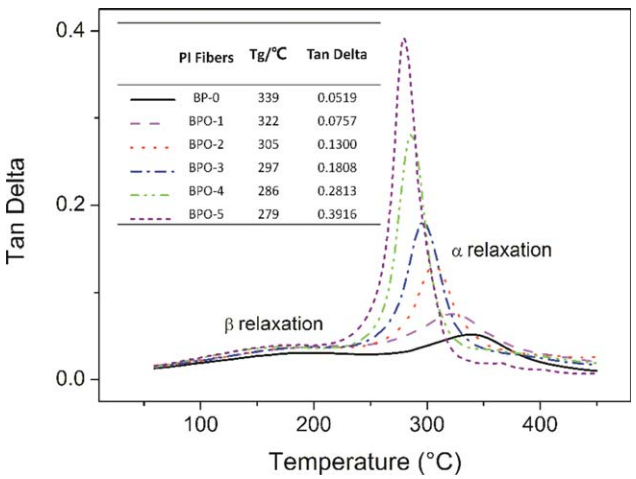

Figure 9. DMA curves of the co-PI fibers with different molar ratios of *p*-PDA/ODA. [Color figure can be viewed in the online issue, which is available at wileyonlinelibrary.com.]

and increased intensities of α relaxations are derived from the improved flexibility of the polymer chains.

CONCLUSIONS

A series of co-PI fibers were prepared by incorporating ODA into the rigid BPDA/*p*-PDA backbone via a two-step wet-spinning method. The processability and mechanical properties of PI fibers were drastically improved with the increased ODA moieties. The optimum mechanical properties of the co-PI fibers were achieved at a *p*-PDA/ODA molar ratio of 5/5 with the tensile strength of 2.53 GPa, almost 3.7 times the strength of homo-PI fibers. Highly oriented structures of PI fibers were identified along the fiber direction, and the optimum degree of molecular orientation of 0.91 was obtained for BPO-1 fibers, while further introducing the ODA contents led to the reduction in the value. Besides, the needle-shaped scattering in SAXS patterns indicated the existence of microvoids in the fibers, and the average radius, length, misorientation of the microvoids were found to decrease with the increased ODA contents, suggesting the gradually formed homogeneous structures in the fibers. The co-PI fibers exhibited excellent thermal stabilities with 5% weight loss temperatures from 563 to 612°C in nitrogen and 536 to 606°C in air and glass transition temperatures from 279 to 339°C. In summary, we provided a new approach in preparing high-performance PI fibers by the two-step wet-spinning method, and the enhancement in mechanical properties was mainly attributed to the gradually formed homogeneous structures in the fibers.

ACKNOWLEDGMENTS

The authors greatly thank the financial support from the National Natural Science Foundation of China (NSFC, Project No.51373008), Higher School Specialized Research Fund for Doctoral Priority Areas of Development Project (No. 20130010130001), and Fundamental Research Funds for the Central Universities of China (Project No. ZY1408).

REFERENCES

1. Cheng, S. Z. D.; Wu, Z. Q.; Eashoo, M.; Hsu, S. L. C.; Harris, F. W. *Polymer* **1991**, *32*, 1803.
2. Dorogy, J. W. E.; Clair, A. K. S. *J. Appl. Polym. Sci.* **1991**, *43*, 501.
3. Dorogy, J. W. E.; Clair, A. K. S. *J. Appl. Polym. Sci.* **1993**, *49*, 501.
4. Zhang, Q. H.; Dai, M.; Ding, M. X.; Chen, D. J.; Gao, L. X. *Eur. Polym. J.* **2004**, *40*, 2487.
5. Yin, C. Q.; Zhang, Z. X.; Dong, J.; Zhang, Q. H. *J. Appl. Polym. Sci.* **2015**, *132*, 41474.
6. Hasegawa, M.; Horie, K. *Prog. Polym. Sci.* **2001**, *26*, 259.
7. Hasegawa, M.; Sensui, N.; Shindo, Y.; Yokota, R. J. Polym. Sci., *Part B: Polym. Phys.* **1999**, *37*, 2499.
8. Dine-Hart, R. A.; Wright, W. W. *J. Appl. Polym. Sci.* **1967**, *11*, 609.
9. Zhuang, Y. B.; Liu, X. Y.; Gu, Y. *Polym. Chem.* **2012**, *3*, 1517.
10. Huang, S. B.; Jiang, Z. Y.; Ma, X. Y.; Qiu, X. P.; Men, Y. F.; Gao, L. X.; Ding, M. X. *Plast. Rubber Compos.* **2013**, *42*, 407.
11. Niu, H. Q.; Huang, M. J.; Qi, S. L.; Han, E. L.; Tian, G. F.; Wang, X. D.; Wu, D. Z. *Polymer* **2013**, *54*, 1700.
12. Dong, J.; Yin, C. Q.; Zhang, Z. X.; Wang, X. Y.; Li, H. B.; Zhang, Q. H. *Macromol. Mater. Eng.* **2014**, *299*, 1170.
13. Liu, J. P.; Zhang, Q. H.; Xia, Q. M.; Dong, J.; Xu, Q. *Polym. Degrad. Stab.* **2012**, *97*, 987.
14. Yin, C. Q.; Dong, J.; Zhang, Z. X.; Zhang, Q. H.; Lin, J. Y. *J. Polym. Sci. Part B: Polym. Phys.* **2015**, *53*, 183.
15. Hasegawa, M.; Sensui, N.; Shindo, Y.; Yokota, R. *Macromolecules* **1999**, *32*, 387.
16. Dong, J.; Yin, C. Q.; Lin, J. Y.; Zhang, D. B.; Zhang, Q. H. *RSC Adv.* **2014**, *4*, 44666.
17. Liang, Y.; Lü, G. Q.; Zhang, J.; Yang, F.; Wu, X. M.; Shan, Y. K. *Acta Chim. Sin. (Chin. Ed.)* **2007**, *65*, 853.
18. Hsiao, S. H.; Chen, Y. *J. Eur. Polym. J.* **2002**, *38*, 815.
19. Snyder, R. W.; Thomson, B.; Bartges, B.; Czerniawski, D.; Painter, P. C. *Macromolecules* **1989**, *22*, 4166.
20. Chang, J. J.; Niu, H. Q.; Zhang, M. Y.; Ge, Q. Y.; Li, Y.; Wu, D. Z. *J. Mater. Sci.* **2015**, *50*, 4104.
21. Lei, X. F.; Qiao, M. T.; Tian, L. D.; Yao, P.; Ma, Y.; Zhang, H. P.; Zhang, Q. Y. *Corros. Sci.* **2015**, *90*, 223.
22. Lei, X. F.; Chen, Y.; Zhang, H. P.; Li, X. J.; Yao, P.; Zhang, Q. Y. *ACS Appl. Mater. Interfaces* **2013**, *5*, 10207.
23. Lei, X. F.; Yao, P.; Qiao, M. T.; Sun, W. L.; Zhang, H. P.; Zhang, Q. Y. *High Perform. Polym.* **2014**, *26*, 712.
24. Ran, S.; Fang, D.; Zong, X.; Hsiao, B.; Chu, B.; Cunniff, P. M. *Polymer* **2001**, *42*, 1601.
25. Chen, X. M.; Burger, C.; Wan, F.; Zhang, J.; Rong, L. X.; Hsiao, B. S.; Chu, B.; Cai, J.; Zhang, L. N. *Biomacromolecules* **2007**, *8*, 1918.
26. Jiang, G. S.; Huang, W. F.; Li, L.; Wang, X.; Pang, F. J.; Zhang, Y. M.; Wang, H. P. *Carbohydr. Polym.* **2012**, *87*, 2012.
27. Jiang, G. S.; Yuan, Y.; Wang, B.; Yin, X.; Mukuze, K. S.; Huang, W. F. *Cellulose* **2012**, *19*, 1075.
28. Ruland, W. *J. Polym. Sci. Part C: Polym. Symp.* **1969**, *1*, 143.